Science of the Total Environment 861 (2023) 160698

Contents lists available at ScienceDirect

Science of the Total Environment

journal homepage: www.elsevier.com/locate/scitotenv

Impacts of a subtropical storm on nitrogen functional microbes and associated cycling processes in a river-estuary continuum

Jingjie Lin [a,b], Anyi Hu [c], Fenfang Wang [a,b], Yiguo Hong [d], Michael D. Krom [e,f], Nengwang Chen [a,b,*]

[a] Fujian Provincial Key Laboratory for Coastal Ecology and Environmental Studies, College of the Environment and Ecology, Xiamen University, Xiamen, China
[b] State Key Laboratory of Marine Environment Science, Xiamen University, Xiamen, China
[c] CAS Key Laboratory of Urban pollutant Conversion, Institute of Urban Environment, Chinese Academy of Sciences, Xiamen, China
[d] Institute of Environmental Research at Greater Bay Area, Guangzhou University, Guangzhou, China
[e] Morris Kahn Marine Station, Charney School of Marine Sciences, University of Haifa, Haifa, Israel
[f] School of Earth and Environment, University of Leeds, Leeds, UK

HIGHLIGHTS

- Increased freshwater discharge resuspended previously deposited sediment.
- The dominant AOA switched from a marine species to a river species (*Nitrosotenuis*).
- The dominant AOB was still the marine genus (*Nitrosomanas*).
- Changed DIN and isotopic composition confirmed active nitrification in water column.
- Abundances of denitrifiers, DNRA and anammox increased while its activity unknown.

GRAPHICAL ABSTRACT

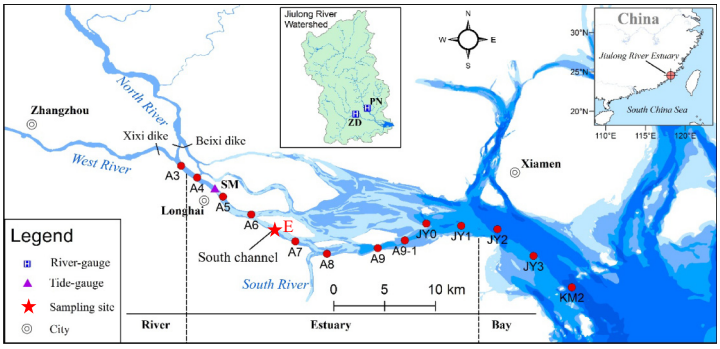

ARTICLE INFO

Editor: José Virgílio Cruz

Keywords:
Storm flow
Nitrogen microbes
Jiulong River estuary
Nitrification
Denitrification
Nutrients

ABSTRACT

Storms, in subtropical regions such as S.E. China, cause major changes in the physical and biogeochemical fluxes of anthropogenic N species through the river-estuary continuum to the coast. Two weeks continuous observations at a sampling station (Station E) in the upper Jiulong River Estuary (S.E. China) were conducted to track the changes of physical and biogeochemical parameters together with genomic identification of nitrogen cycling microbes through a complete storm event in June 2019. In conjunction with previous N flux measurements, it was found that there was greatly increased flux of N to and through the upper estuary during the storm. During the storm, the freshwater/brackish water boundary moved downstream, and previously deposited organic rich sediment was resuspended. During baseflow, anthropogenically derived ammonium was oxidised dominantly by the marine nitrifying (AOA) microbe *Nitrosopelagicus*. However, during the storm, the dominant ammonia-oxidizing archaea (AOA) at Station E changed to the riverine genus (*Nitrosotenuis*) while the marine genus, *Nitrosopumilus* decreased. At the same time the dominant ammonia-oxidizing bacteria (AOB) was still the marine genus (*Nitrosomanas*). Estuarine nitrifiers had higher abundance, weighted entropy and diversity during the Flood, suggesting that the high NH_4-N and DO during the Rising period of the Flood resulted in a bloom of nitrifiers. The changing gene abundances of nitrifiers were reflected in changes in the concentration and isotopic composition of DIN confirming active nitrification in the oxygen-rich water column. During the storm the numbers of denitrifiers (*nar*G, *nir*S and *nod*), DNRA (*nrf*A) and anammox (*hzs*B) were found in the water column increased, and the larger fraction was associated with the <22 μm free-living fraction. However it was not possible with the data obtained to estimate what fraction of these anaerobic bacteria were active in the dominantly oxic water column.

* Corresponding author at: College of the Environment and Ecology, Xiamen University, Xiamen 361102, China.
E-mail address: nwchen@xmu.edu.cn (N. Chen).

http://dx.doi.org/10.1016/j.scitotenv.2022.160698
Received 23 August 2022; Received in revised form 26 September 2022; Accepted 1 December 2022
Available online 6 December 2022

1. Introduction

Climate change will likely cause an increase in the number and intensity of storms that will result in major pulses of increased freshwater discharge. As a result of such storms there will be a higher flux of watershed materials including soil particles with attached pollutants and anthropogenic nutrients into rivers and estuaries and from there into offshore systems (Brown et al., 2013; Chen et al., 2018a; Surbeck et al., 2006). An important component of this storm enhanced discharge is anthropogenic nitrogen (N) and the microbes that can transform one type of N compound to another. For example, 42–47 % of the total annual discharge of ammonium and nitrate N from the Jiulong River (China) watershed, most of which was derived from wastewater discharge, occurred during a few storm events in 2014 (Gao et al., 2018). As a result of the high river discharge during storms, additional particle-attached and free-living microbes are transported downstream to the estuary and thence to the coast from terrestrial sources, including from point-source and non-point source wastewater discharges and resuspended and eroded riverine and upper estuarine sediments (Jamieson et al., 2005; Jeng et al., 2005). These inputs of exogenous microorganisms can cause major changes in the composition and function of microbial communities in the river system and downstream in the estuary and coastal waters (Chi et al., 2021; Nakatsu et al., 2019; Nevers et al., 2020). For example it was found that riverine benthic nitrifying activity was reduced during storm flow, as surface sediments with nitrifiers were removed (Cooper, 1983). Downstream, particularly in the upper estuary which during the storm is freshwater, N cycling microbial assemblages, can result in changes in the amount and nature of nitrogen loading being fluxed through the estuary to the coast (Fortin et al., 2021; Lin et al., 2020; Wang et al., 2022; Yan et al., 2019; Lin et al., 2022). However, detailed information of how N cycling microbial communities change during flood disturbance events through a major particle-rich river-estuary continuum is understudied.

Microbial N cycling processes in the river-estuary systems include nitrification, denitrification, dissimilatory nitrate reduction to ammonia (DNRA) and anaerobic ammonium oxidation (anammox). Nitrification oxidizes ammonium to nitrate via nitrite, which is mediated by the first step of ammonia-oxidizing archaea (AOA) and ammonia-oxidizing bacteria (AOB) and the second step of nitrite-oxidizing bacteria (NOB) (Galloway et al., 2008; Konneke et al., 2005; Sorokin et al., 2012). An important N removal process is microbially driven denitrification, in which nitrate/nitrite is reduced to N_2O and N_2 mediated by *nar* (nitrate reductase), *nir* (nitrite reductase), *nor* (nitric oxide reductase) and *nos* (nitrous oxide reductase) genes (Warneke et al., 2011). DNRA, an alternative microbial reduction process, reduces nitrate/nitrite to ammonium and is beneficial as it reduces the emissions of the potent greenhouse gas N_2O, which occurs as a biproduct during microbial denitrification (Pandey et al., 2020). Anammox converts ammonium and nitrite to dinitrogen gas resulting in N removal from the river-estuary system (Hou et al., 2013; Kartal et al., 2011). Considering high ammonium and nitrate concentration in the Jiulong river-estuary system, these microbial processes can play an important role in the turnover of N nutrients.

The effects of storms and how they affect variations of N concentrations and fluxes across the river-estuary-coast continuum have been studied in a number of different river systems (Blanco et al., 2010; Chen et al., 2018a; Chen et al., 2012; Gao et al., 2018; Lin et al., 2022). However, there is limited information about how flood events alter the microbial community and their genetic makeup through the river-estuary systems including how these changes impact N cycling and export through the estuary system. In this study, we investigated the changes in hydrological conditions, N species (ammonium, nitrate and nitrite), N functional genes (nitrification, denitrification, DNRA and anammox) and 16S rRNA genes as well as community composition and diversity of ammonia-oxidizing microbes during a complete flood event (June 2019) in the upper Jiulong River Estuary (JRE). We consider JRE as an example of a typical particle rich river system which is affected by considerable anthropogenic inputs of pollutant N species. The specific objectives of the study were to: (1) explore the storm-induced changes in the community and abundance of nitrifiers and the resulting N chemical species produced; and to (2) explore the storm-induced changes in particle-attached (PA) and free-living (FL) N cycling microbes, which change their niche after riverine particle inputs mix with resuspended sediments that had been temporarily deposited in the upper estuary during periods of normal flow and are then resuspended and advected downstream together during the storm.

2. Methods

2.1. Study area

The Jiulong River Estuary (JRE; Fig. 1) receives discharge mixing agricultural and residential wastewater from point and non-point sources. It is the second largest river in Fujian province of China, and 90 % of the estuarine discharge exports to Xiamen Bay and thence to the Taiwan Strait from its southern channel (Chen et al., 2018a; Lin et al., 2020). The subtropical monsoon climate in the region causes high precipitation and temperature, between May to August, including storms and occasionally typhoons. As a semi-enclosed macrotidal estuary, the JRE has 2–3 days of average flushing time, 2.7–4 m tidal range, 0–30 ‰ salinity gradient and 3–16 m depth (Cao et al., 2005). The fixed sampling Station E (Fig. 1) is in the core area of the Estuarine Turbidity Maximum (ETM) with 0–5 ‰ salinity gradient during normal baseflow condition (Lin et al., 2022; Yu et al., 2020; Yu et al., 2019).

2.2. Sampling campaign

The sampling campaign was designed to capture in detail a major storm/flood event, which took place between June 10th and 23rd 2019. Hourly river discharge was obtained from the local government measurements at the closest hydrological stations in the North and West rivers respectively (PN and ZD, Fig. 1) adjusted to include estimates of the additional flux to the rivers downstream of the gauging stations (Lin et al., 2022). The values given here are the sum of the discharges of both rivers together into the estuary. The sampling was divided into Initial, Rising, Falling and Ending phases based on the observed river discharge (Fig. 2a). The flood event was also divided into Baseflow (Initial and Ending) and Flood defined as >1.2 times the baseflow (Rising and Falling). In order to collect samples during complete tidal cycle, water samples were collected at Station E every 2 h, during 10 tidal cycles each lasting 14 h (11th to 17th, 19th, 21st and 23rd).

We collected nutrient samples (0.5 L) and genome samples (1 L) at the same time, using by a 5 L plexiglass sampler under 0.5 m depth at a point several meters away from the bank to ensure the samples were from the main estuary flow. Each water sample was filtered using GF/F (0.7 μm) filters and placed in fridges at 4 °C, and filter membranes were placed in fridges at −20 °C. All samples were transported to the lab in Xiamen University every three days for subsequent analysis.

An in-situ sensor (Aqua TROLL 600, USA) was fixed in the bottom water of Station E (1 m above surface sediment) which measured hourly dissolved oxygen (DO), water temperature, turbidity and pH.

2.3. Chemical analysis

SPM was the difference between the unfiltered and filtered membranes after oven-drying (105 °C) to constant weight. The filtrate was analyzed for ammonium (NH_4-N), nitrate (NO_3-N), and nitrite (NO_2-N) by segmented flow automated colorimetry (San++ analyzer, Germany) within one week of sampling. The precision of analysis determined by repeated sampling of 10 % of the samples was <5 % relative error. Total dissolved nitrogen (TDN) was determined as NO_3-N following oxidization with 4 % alkaline potassium persulfate. Dissolved organic nitrogen (DON) was calculated by subtracting DIN from TDN.

2.4. Molecular analysis

The samples for genome determination were first filtered by a 20 μm bluteau filter to remove large particles and algae. In order to distinguish

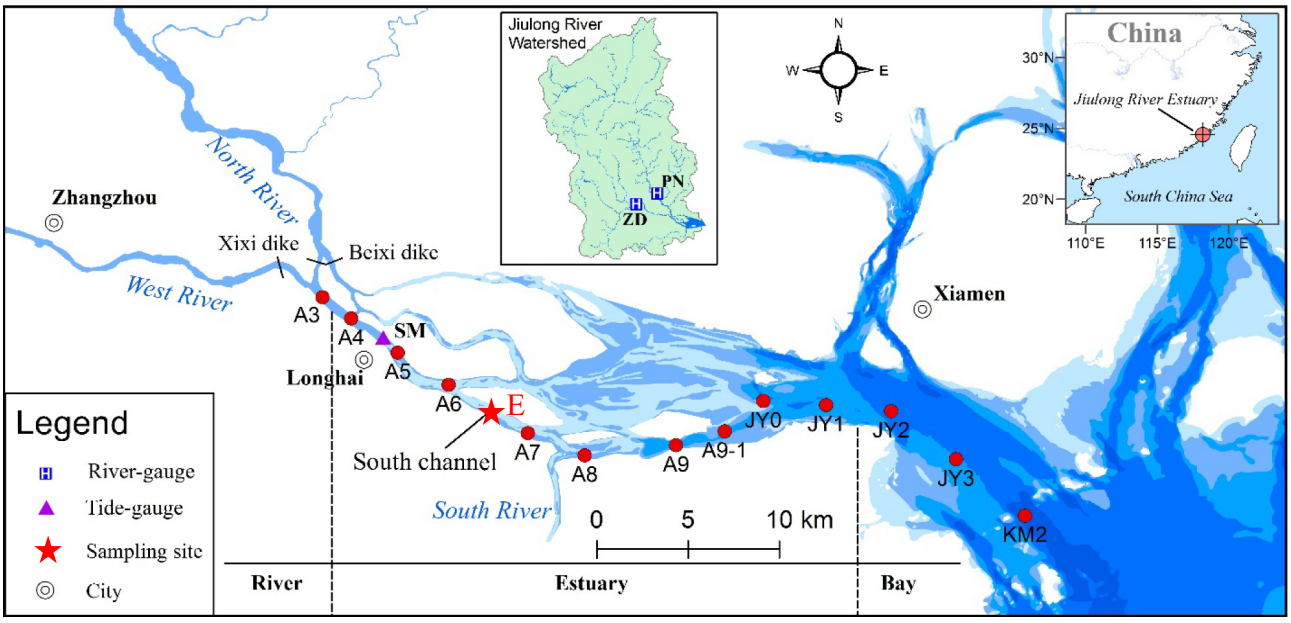

Fig. 1. Map of the Jiulong River Estuary showing the fixed estuary site (E) and the tide gauge site at Shima (SM). Light blue indicates shallow water. Red circles are the stations sampled regularly in previous studies (Chen et al., 2018a; Chen et al., 2018b; Yu et al., 2019; Lin et al., 2022). PN and ZD in the insert map are the hydrological stations used to determine the water discharge and nature of chemical species fluxing out of the North and West river in these previous publications.

between the relative abundances of particle-attached (PA) and free-living (FL) microbes, one sample per day sampled at low tide was filtered by 3 μm and 0.22 μm Isopore TM Membrane (47 mm, Millipore, USA), respectively. The sum of PA and FL abundances was equal to the total abundance. DNA was extracted using FastDNA Spin Kit for Soil (Millipore, USA). The quantitative PCR (qPCR) amplification of microbial N functional genes was performed using a Bio-Rad CFX96 qPCR system (Bio-Rad Laboratories, Inc., USA). Primer pairs and amplification protocols for qPCR (archaeal *amo*A, bacterial *amo*A, *nxr*A, *nar*G, *nir*S, *nod*, *nrf*A, *hzs*B and 16S rRNA) are shown in Table S1 and S2, respectively. To characterize the community dynamics of AOA and AOB, the archaeal and bacterial *amo*A genes were sequenced for four flood phases samples on an Illumina MiSeq instrument using 2 × 300 bp lengths with a total of 40–50 K reads by the company GENEWIZ (China). To ensure the quality and limit of detection of the gene analysis, we evenly mixed equal amount of PA and FL samples for high-throughput sequence. The high-throughput sequencing data were analyzed using Mothur v.1.35.1 (Schloss et al., 2009). For more details of the procedures used see Lin et al. (2020). The raw Illumina reads of *amo*A gene sequences were deposited in the National Center of Biotechnology Information (NCBI) in accession NO. PRJNA656067 (AOA) and NO. PRJNA656066 (AOB).

2.5. Auxiliary data, calculation and statistical analysis

Hourly river discharge at the closest hydrological stations (PN and ZD, Fig. 1) was gathered from local government data. The tidal range at the Shima tide-gauge was obtained from the National Maritime Information Service (https://www.cnss.com.cn/tide/). A complimentary data set of nutrient

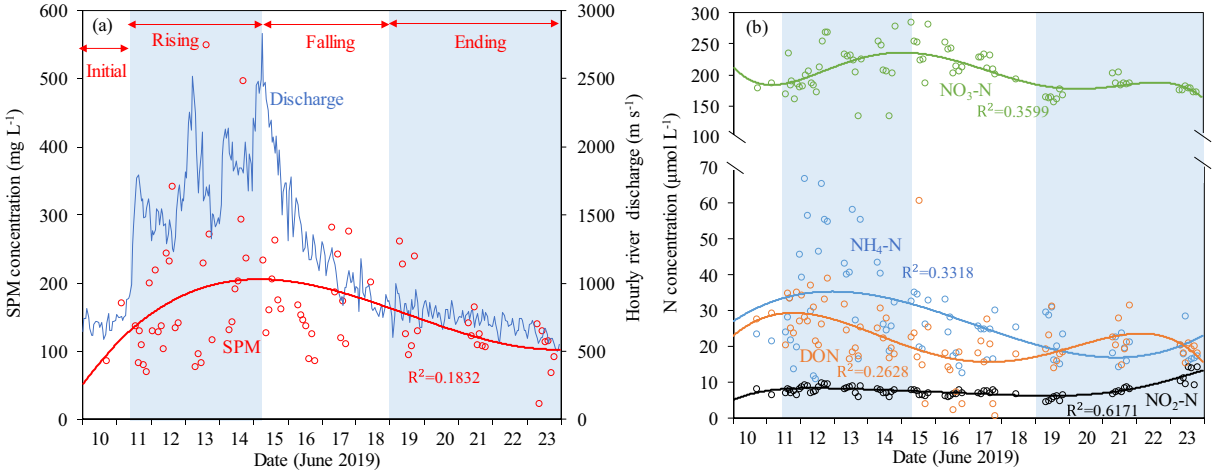

Fig. 2. Plot 2(a) shows the hourly river discharge as calculated in Lin et al., 2022 from local government measurements at the closest hydrological stations (ZD and PN) corrected for additional discharge into the lowest reaches of the river and SPM measured by discrete sampling at Station E during the four periods of the storm. The storm was divided into Initial, Rising, Falling and Ending based on the nature of the measured discharge rate. For more details of the discharge conditions see Lin et al. (2022). Plot 2(b) shows the measured concentrations of dissolved N species at Station E during the same sampling period.

concentrations, isotopic ratios and calculated N flux was collected at two stations at the exit of the North (NJR) and West (WJR) rivers during this storm (Lin et al., 2022). For details of Statistical analyses used see Supplementary Information.

3. Results

3.1. Physiochemical changes during the flood event

At the beginning of the storm (Initial) Station E was at or close to the location of the boundary between fresh and brackish water, which was considered to be the ETM. The resuspension processes at the ETM were controlled by the tidal cycle (Fig. S1). As the storm and the river discharge increased (Rising and Falling), the freshwater-brackish water boundary moved downstream, and Station E was occupied by freshwater during the entire tidal cycle. At the same time the water depth increased by 12 cm while the tidal range decreased by 26 cm (Table 1). During the period of high river discharge (Rising and Falling), the physiochemical characteristics of the water at Station E were close to that of the lowest parts of the North and West river with lower water temperature, higher DO and lower pH (Fig. 3). Both SPM and turbidity were significantly higher during high flow (K—S test, $P < 0.05$), which had peak values during the Rising (Fig. 2a, Fig. 3c).

All species of inorganic N increased in concentration during the flood event (Fig. 2b). The average concentration of DIN increased from 213 μmol L^{-1} in the Initial to ~255 μmol L^{-1} during the Rising and Falling (Table 1), while the minimum concentration in the Baseflow was 182 μmol L^{-1} increasing to a maximum of 334 μmol L^{-1} in the Flood period (Fig. 2). Most of the additional DIN came as NO_3-N (84.9 ± 4.4 % of DIN), with a smaller fraction (12 ± 4.3 % of DIN) as NH_4-N. Together these two species made up 91.5 ± 3.2 % of TDN. DON had a minor decrease from 28.6 μmol L^{-1} in the Initial to 26.4 μmol L^{-1} in the Rising, and then decreased further to 20.7 μmol L^{-1} in the Ending (Table 1). The peak value of NH_4-N was measured in the middle of Rising, while the peak of NO_3-N was somewhat later at the Rising-Falling transition (Fig. 2b). A minor peak of NO_2-N (8.2 ± 1 μmol L^{-1}) was measured in the Rising, while the major peak of NO_2-N (8.6 ± 3 μmol L^{-1}) was found at the end of Ending (Table 1, Fig. 2b).

Table 1
Physiochemical changes at Station E during the storm.

Parameter (unit)	The storm event (June 10th to 23rd 2019)			
	Initial	Rising	Falling	Ending
Hourly river discharge (m^3 s^{-1})	699.1 ± 53.6 ^{c}	1679.2 ± 410.8 ^{a}	1360.9 ± 443.7 ^{b}	737 ± 96.3 ^{c}
Water depth (cm)	468.1 ± 144.3 ^{b}	480.4 ± 123.5 ^{a}	472.9 ± 147.5 ^{a}	466.3 ± 135.8 ^{b}
Tide range (cm)	275 ± 5.7 ^{a}	268.7 ± 7.2 ^{a}	275 ± 5.2 ^{a}	247.8 ± 10.1 ^{b}
Water temperature (°C)	26.7 ± 0.3 ^{a}	25 ± 1 ^{b}	25 ± 0.6 ^{b}	27.3 ± 0.8 ^{a}
DO (%)	67 ± 4.5 ^{d}	70.4 ± 5.1 ^{c}	76.9 ± 6.5 ^{a}	73.2 ± 4.8 ^{b}
pH	7.2 ± 0.1 ^{b}	7.1 ± 0.1 ^{c}	7.1 ± 0.2 ^{c}	7.3 ± 0.1 ^{a}
SPM (mg L^{-1})	129.5 ± 59.4 ^{b}	187.5 ± 112.5 ^{a}	171.8 ± 57.2 ^{a}	129.9 ± 57.1 ^{b}
DON (μmol L^{-1})	28.6 ± 1.2 ^{a}	26.4 ± 6.5 ^{a}	17.2 ± 12.6 ^{b}	20.7 ± 4.8 ^{a}
DIN (μmol L^{-1})	212.8 ± 3.7 ^{b}	254.4 ± 112.5 ^{a}	256.5 ± 28.1 ^{a}	206.4 ± 12.2 ^{b}
NH_4-N (μmol L^{-1})	22.6 ± 1.4 ^{b}	36.1 ± 15.8 ^{a}	24.2 ± 6.8 ^{b}	20.8 ± 5.1 ^{b}
NO_3-N (μmol L^{-1})	182.5 ± 6.2 ^{b}	210 ± 39 ^{b}	225.1 ± 23.5 ^{a}	177 ± 12.6 ^{c}
NO_2-N (μmol L^{-1})	7.7 ± 1.2 ^{c}	8.2 ± 1 ^{b}	7.2 ± 0.6 ^{c}	8.6 ± 3 ^{a}
NH_4-N/DIN (%)	10.7 ± 0.8 ^{b}	13.9 ± 4.5 ^{a}	9.4 ± 2 ^{b}	10.1 ± 2.7 ^{b}
NO_3-N/DIN (%)	85.7 ± 1.5 ^{a}	82.8 ± 4.5 ^{b}	87.8 ± 1.9 ^{a}	85.8 ± 2.3 ^{a}
NO_2-N/DIN (%)	3.6 ± 0.6 ^{b}	3.3 ± 0.4 ^{b}	2.8 ± 0.4 ^{c}	4.1 ± 1.3 ^{a}
DON/DIN	0.13 ^{a}	0.11 ± 0.03 ^{a}	0.07 ± 0.05 ^{b}	0.1 ± 0.02 ^{a}

Note: a, b, c and d represent significant differences ($P < 0.05$) among the four phases of the storm event (Initial, Rising, Falling and Ending).

3.2. Changes of the abundances of microbial N functional genes during the flood event

The total abundances of microbial N functional genes (sum of PA and FL) showed major changes during the Flood (Fig. 4, Table S4). The abundances of the nitrifying genes *amo*A (AOA), *amo*A (AOB) and *nxr*A (NOB) significantly increased by an average of 1.4, 3.6 and 2.2 times during the Flood (Rising and Falling) as compared to the abundances of 1.3×10^3 copies mL^{-1}, 1.8×10^3 copies mL^{-1} and 2.4×10^3 copies mL^{-1} respectively during the Initial. For the denitrifying genes, the abundances of *nar*G and *nir*S decreased during the Flood to 3.0–1.3 $\times 10^5$ copies mL^{-1} and 3.5–3.2 $\times 10^5$ copies mL^{-1} as compared to the abundances of 2.4×10^5 copies mL^{-1} and 4.7×10^5 copies mL^{-1} during the Initial (i.e. Baseflow). The abundances of anammox gene (*hzs*B) and DNRA gene (*nrf*A) both increased 1.3 times during the Flood compared with the abundances of 1.7×10^4 copies mL^{-1} and 7.0×10^7 copies mL^{-1} during the Initial. The response time of nitrifying functional genes to reach maximum abundance, (*amo*A (AOA) and *nxr*A (NOB)) was faster than *amo*A (AOB) (Fig. 4). In addition, the ratio of *nxr*A/*amo*A increased from 1.8 (Initial) to 2.9 (Rising).

Our results showed that the amount and relative proportion of free-living N functional genes increased considerably during the progress of the storm, especially for the nitrifiers (Fig. 4, Fig. 5). The nitrifying gene *nxr*A (NOB) and 16S rRNA genes had higher relative abundance in FL than in PA (FL/PA > 1; Table S4). The ratios of FL/PA of nitrification, DNRA, anammox and 16S rRNA genes all increased by a factor of more than one during the Flood. This effect was particularly large for *amo*A (AOB) which increased by 9 times (Table S5). By contrast, the denitrifying genes (*nar*G and *nir*S) still had higher abundances in PA than in FL (FL/PA ratios <1) through the Flood period. The response time of maximum FL abundances, showed different patterns for different N functional genes (Fig. 5). For example, for nitrifying genes the response time of *amo*A (AOA) was shorter than *amo*A (AOB) and *nxr*A.

3.3. Diversity, variation and probability of interspecific encounter in N functional species

During the flood event, the Shannon-Wiener, Simpson's diversity and PIE indexes of N functional genes decreased from 1.28 to 0.24, 0.51 to 0.06 and 2.03 to 1.07, respectively (Fig. 6). The N functional genes at the transitional period of Rising-Falling had the lowest diversity and PIE indicating the minimum evenness among N functional microbes. As for variation of the absolute abundances of such genes, nitrifying *amo*A (AOB) had the minimum value of entropy (Ep) and the maximum value of weighted entropy (Wp) as compared to other N functional and 16S rRNA genes (Fig. 6d).

3.4. Community composition and diversity of ammonia-oxidizing microbes (AOA and AOB)

Overall, high-quality reads of *amo*A genes obtained for AOA and AOB, respectively, were clustered into *amo*A (AOA) and *amo*A (AOB) at a cutoff of 97 % identity after sub-sampling. The results of rarefaction curves indicated the current sequencing depth was able to fully describe the composition and diversity of AOA and AOB communities (Fig. 7). At Station E, the α-diversities of AOA and AOB communities were comparable between the flood event in June 2019 and normal baseflow period in November 2018 (Fig. 7c, d). Both AOA and AOB reached the maximum diversity (e.g., the highest Shannon-Weiner) and richness (e.g., the highest OTUs and Chao1) during the Rising and Falling (Table 2).

Community composition of AOA at Station E tended to shift to the riverine pattern during the flood event (Fig. 7a). During the Initial phase which is before the storm, the dominant genus of AOA communities in water of the JRE and Jiulong River was *Nitrosopelagicus* (62.3 %, marine genus) and *Nitrosotenuis* (55.8 %, freshwater genus), respectively. During the flood, *Nitrosotenuis* was found at Station E, which had higher relative

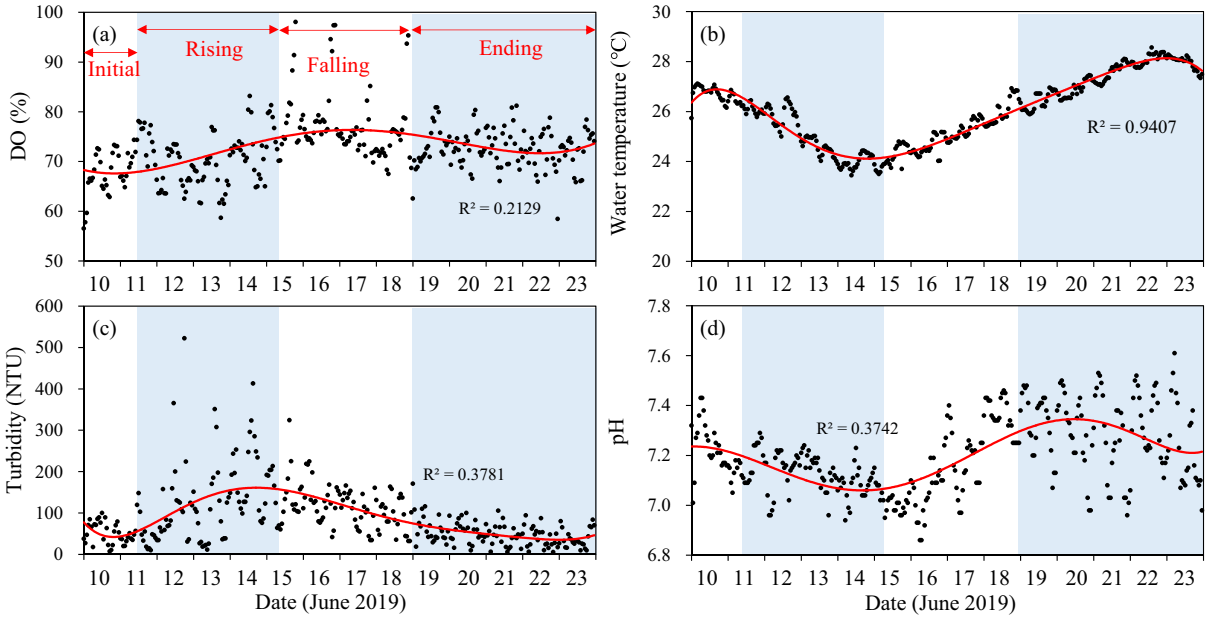

Fig. 3. Temporal distribution of (a) Dissolved Oxygen (DO), (b) Water temperature, (c) turbidity and (d) pH measured during the storm at Station E by the In-Situ sampler.

abundance (10.4 % vs. 0.7 %) at low tide than at high tide and increased to 31.2 % during the Rising. The freshwater genus of *Nitrosotalea* was also found at Station E during the Flood, while the marine genera of *Nitrosopelagicus*, *Nitrosopumilus* and *Nitrosomarinus* decreased or disappeared.

The Community composition of AOB in the JRE had some variation during the Flood, compared with the Initial Baseflow (Fig. 7b). *Nitrosomonas* was the dominant genus (82.8 %) in water column both in the JRE and Jiulong River, while *Nitrosospira* was the dominant genus (35.5 %) in sediments and soils of the Jiulong River. During the Initial phase, AOB in the JRE had higher relative abundance of *Nitrosospira* (30.5 %). However, *Nitrosomonas* (87.4 %) became the dominant AOB in the JRE during the Rising.

4. Discussion

4.1. Changes in physical conditions through the storm

The changes in the hydrological and sedimentological conditions in the upper estuary of the Jiulong river-estuary system are described in detail in Lin et al. (2022). Here we present a summary of the most important changes needed to understand the changes in nutrient chemistry and gene abundances caused by the storm in June 2019. During normal baseflow conditions, the freshwater-brackish water boundary and the resultant ETM is found at Station E (Yu et al., 2019). As the river discharge increases, this boundary moves down the estuary such that during the peak of the flood

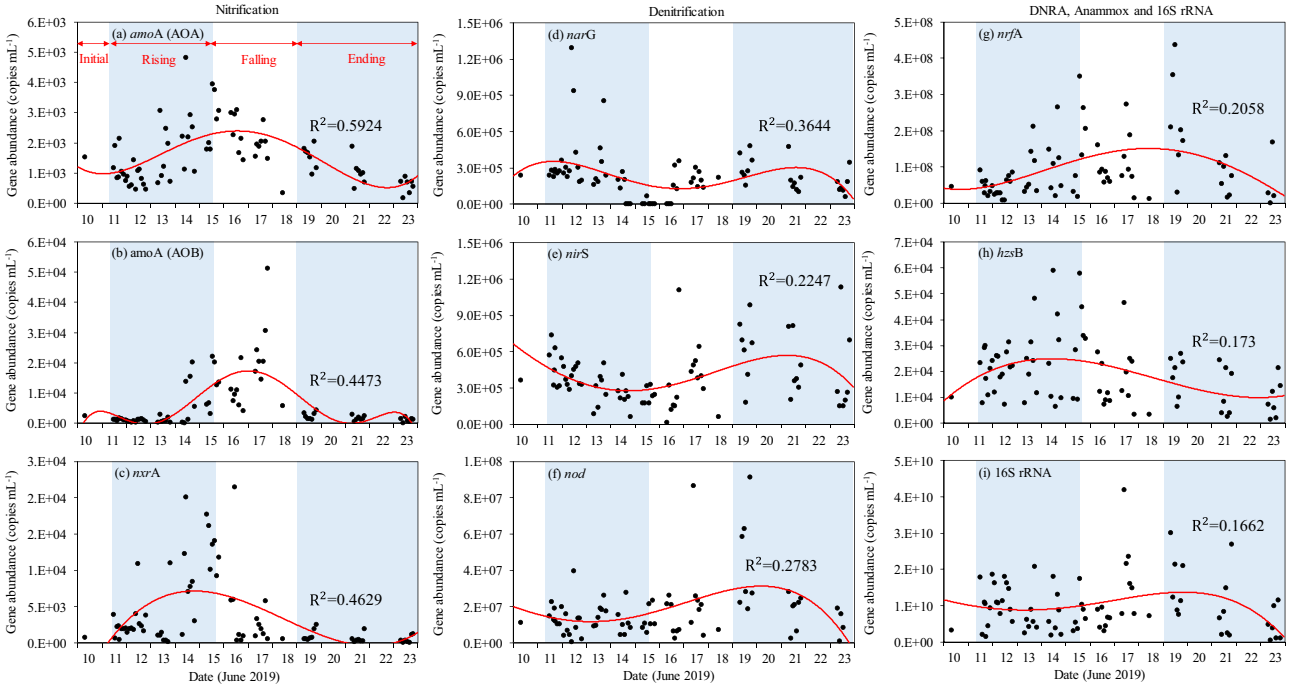

Fig. 4. Hourly distribution of gene abundances (copies mL^{-1}) measured during the storm at Station E.

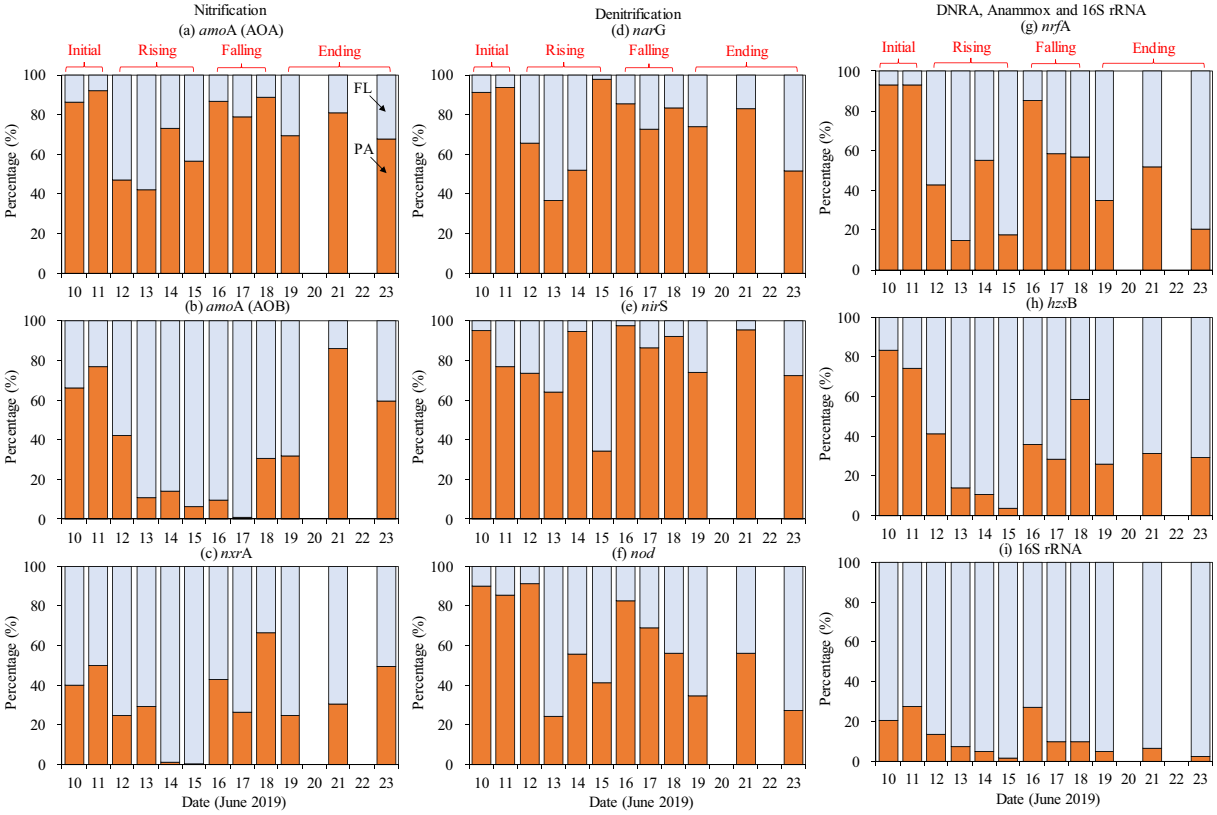

Fig. 5. Distribution of particle-attached (PA) and free-living (FL) gene abundances during the storm event at Station E. The percentage of PA gene abundances is shown in orange column, while the percentage of FL gene abundances is shown in blue.

it is downstream of Station E. As a result, the water at Station E during the Rising and Falling is characteristically freshwater with lower temperature and pH (Table 1). In addition the speed of flow of that water is higher than during the Baseflow (Lin et al., 2022). As the river discharge decreased, the freshwater-brackish water boundary moved back upstream again and at Station E there is again a tidal change between freshwater at low tide and brackish water at high tide (Fig. S1). Thus Station E represents the upper boundary of the brackish water under normal flow. During flood

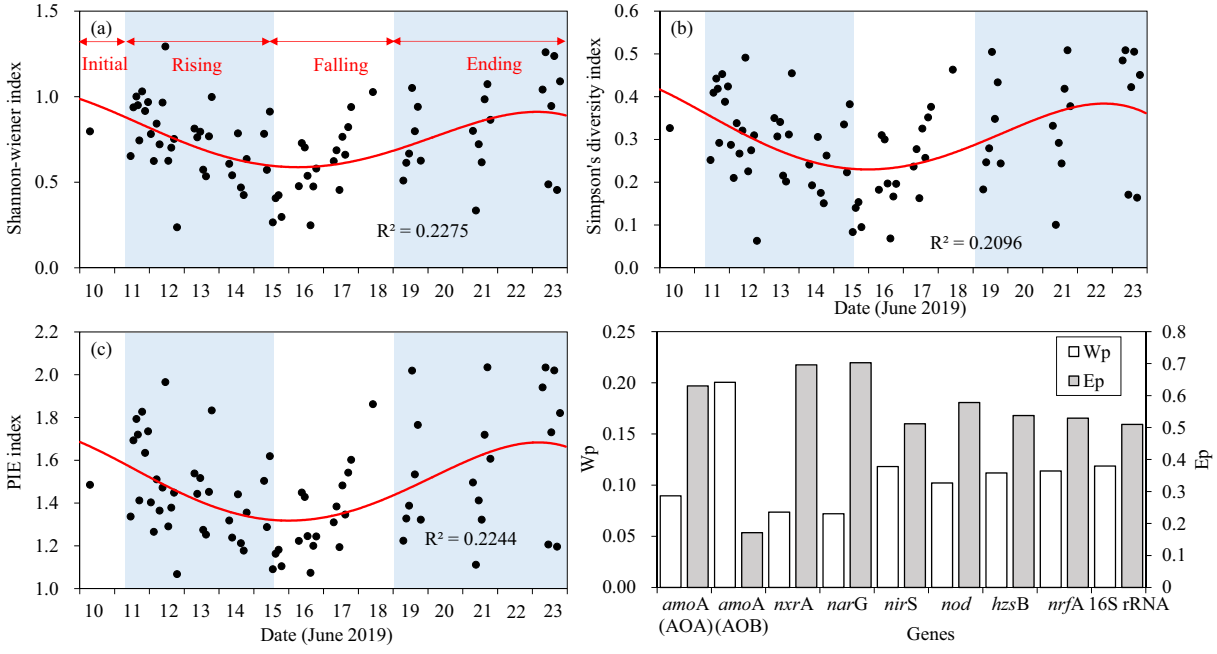

Fig. 6. (a) The Shannon-Wiener index, (b) Simpson's diversity index, (c) PIE index, (d) Wp (Weighted entropy) and Ep (Entropy) of nitrogen functional genes during the storm.

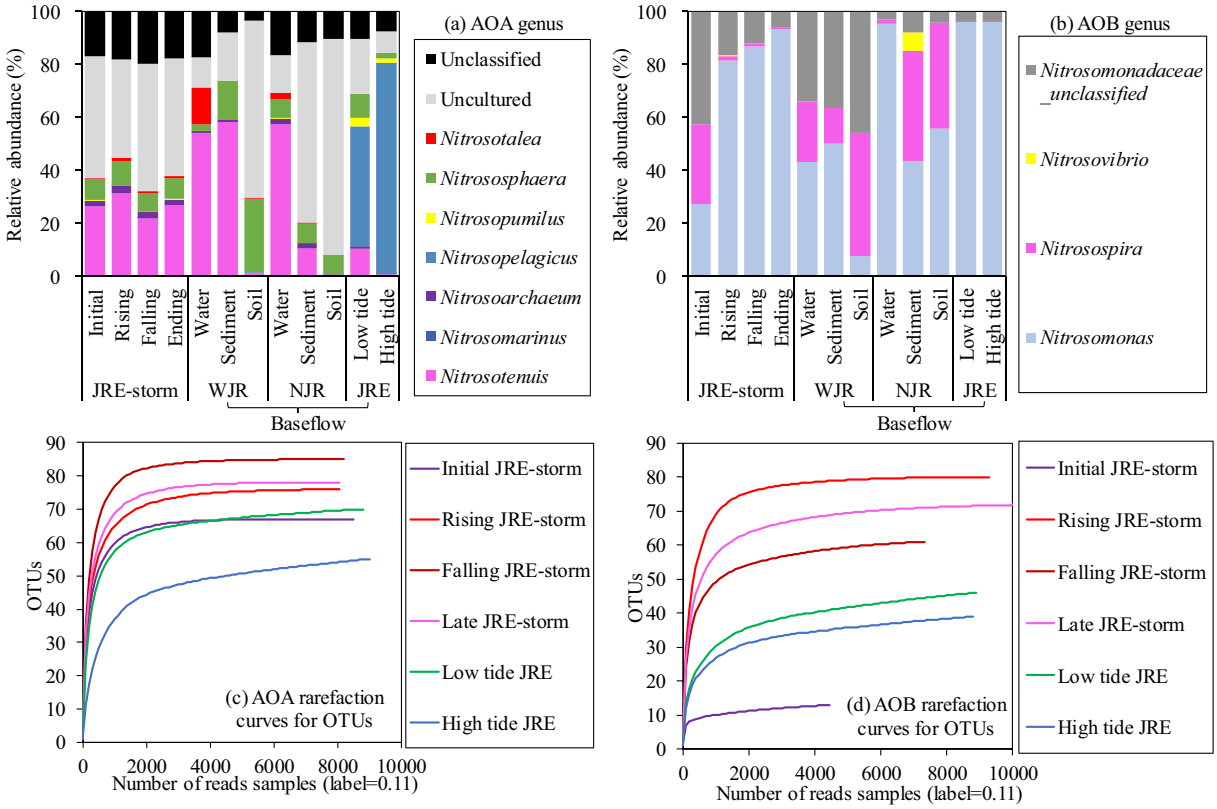

Fig. 7. Relative abundances of communities of (a) AOA and (b) AOB during the storm of June 2019, and during normal baseflow measured in November 2018 in the water, sediment and soil of West Jiulong river (WJR), North Jiulong river (NJR) and Jiulong river estuary (JRE). Rarefaction curves for (c) AOA and (d) AOB for Operational Taxonomic Units (OTUs) in the JRE based on 97 % cut-offs. The data in water, sediment and soil of WJR, NJR and JRE during normal baseflow is from Lin et al. (2020).

conditions there were major increases in chemical fluxes and changes in microbial community caused by storm flooding.

It has been shown (Lin et al., 2022; Yu et al., 2019), that during normal flow, sediment containing labile organic matter and characteristic freshwater bacteria is deposited temporarily in the estuary upstream of Station E. Previous works (Lin et al., 2022; Yu et al., 2020; Zhang et al., 2022) has suggested that during the temporary deposition of this sediment, diagenetic reactions occur which are characteristic of estuarine brackish water conditions. During the peak of the flow there was an increase in SPM (Fig. 3c). This SPM has been shown to include eroded sediment and soil washed into the rivers which is carried downstream into the estuary, plus that fraction of the temporarily deposited sediment resuspended by the flood waters. It is these sediment particles with their associated microbes that become entrained in the water column and were sampled during the peak of the flood at Station E (Fig. 4).

Table 2
The alpha diversity index of AOA and AOB in the Jiulong River estuary.

Gene	Sample	Coverage	Simpson	Chao1	Shannon	Ace	OTUs
*amo*A (AOA)	Initial	100 %	0.08	67	3.17	67	67
	Rising	100 %	0.07	76	3.26	76	76
	Falling	100 %	0.07	85	3.40	85	85
	Ending	100 %	0.07	78	3.29	78	78
	Low tide-baseflow	100 %	0.26	74	2.33	72	70
	High tide-baseflow	100 %	0.72	70	0.91	60	55
*amo*A (AOB)	Initial	100 %	0.29	16	1.48	17	13
	Rising	100 %	0.07	80	3.20	80	80
	Falling	100 %	0.09	62	2.88	62	61
	Ending	100 %	0.11	72	2.88	72	72
	Low tide-baseflow	100 %	0.19	46	2.08	45	46
	High tide-baseflow	100 %	0.22	38	1.89	38	39

4.2. Dynamic changes in gene abundances and N chemistry characteristic of nitrification

The community of AOA at Station E in the estuary measured in the drier season of November 2018 was very different in diversity both from the river in November 2018 (Lin et al., 2022) and during the entire storm including baseflow during the summer wet season (June 2019 (Fig. 7). In November 2018, the dominant AOA genus in the JRE was the marine genus *Nitrosopelagicus* while in the river it was the freshwater genus *Nitrosotenius*. The reason for this was that at that time the total river discharge was much lower than in June 2019. As a result both the freshwater/brackish water boundary and the ETM were upstream of Station E (Yu et al., 2019). In the Jiulong estuary as in many similar estuaries, the ETM is a location of high sediment resuspension and high oxygenation (Yu et al., 2020). The water column at and below the ETM including at Station E in November 2018 was dominantly brackish (Yan, 2012). This is a location where dissolved anthropogenically derived ammonium being brought down the river is oxidised by AOA with the marine nitrifying bacteria *Nitrosopelagicus* dominant (Fig. 7a). By contrast the genus diversity in the freshwater part of the Jiulong River in November 2018 and during the entire storm at Station E (JRE) in June 2019 was mainly freshwater genera such as *Nitrosotenius* (Fig. 7a). These freshwater genera also included the genus *Nitrosotalea*, which has been found to be dominant in acidic agricultural areas of the West Jiulong river (Lin et al., 2022). At the same time the marine genus *Nitrosopumilus*, which was reported to occur in the JRE (Zou et al., 2020), decreased during the Flood. The appearance of these

freshwater genera even during the Initial baseflow part of the storm in June 2019, implies that during the summer wet monsoonal season, AOA in the upper estuary is dominated by freshwater genera and the switch to marine genera is probably downstream of Station E even in baseflow. This is consistent with the known salinity changes and other chemical changes at Station E (Table 1) which showed that even during baseflow the water column was dominantly freshwater with only a minor amount of brackish water at high tide (Lin et al., 2022).

It is known that there was a major input of resuspended surficial sediments into the water column during the Rising (Lin et al., 2022) from sediments that had been deposited in brackish water in the upper estuary (Chen et al., 2018b; Cheng et al., 2021; Zhang et al., 2022) during normal flow. It is likely that these sediments had developed a brackish/marine bacterial fauna (Luo, 2014). Yet there was no evidence of this in the water column above Station E during the Flood. It is known that the maximum nitrifying rate in sediment cores from other estuaries is often restricted to a rather thin layer close to the surface (Hou et al., 2007; Meyer et al., 2008). The data presented here suggests that there were not enough marine nitrifying bacteria in the resuspended sediments to change the overall diversity of AOA bacteria which was dominated by freshwater genera during the Flood (Table S5).

The pattern of AOB was somewhat different from AOA. In the drier season of November 2018, *Nitrosomonas* was the dominant genus in the water column in the JRE unchanged from the diversity in the water column of NJR (Fig. 7b), which was the dominant source of water at that time i.e. the dominant genus kept its niche despite the switch from fresh to brackish water (Luo, 2014). The only change in AOB was during the Baseflow (Initial) before the Flood in June 2019, when the genera included *Nitrosospira* and *Nitrosovibrio*, which were found in sediment and soil in the river catchments suggesting that during the wet season there was a contribution from washed and eroded river sediment (Lin et al., 2022). As the flow increased these genera were reduced considerably presumably due to dilution by the dominant genus in river water, *Nitrosomonas*. It has been reported that *Nitrosomonas* can utilize high ammonium in a sludge reactor (Bollmann et al., 2002; Wagner et al., 1996). The high concentration of ammonium upstream during the Flood (Fig. 2b) is likely to support the observed bloom of *Nitrosomonas* at Station E in the JRE.

Estuarine nitrifiers became more abundant among the N functional microbes, when between-community evenness decreased (Fig, 6a, b& c) and within-community diversity increased (Table 2). Higher nitrifying copies (Fig. 4a, b &c) during the Flood, suggesting that the high NH_4-N (Fig. 2b) and DO (Fig. 3b) during the Rising period of the Flood resulted in a bloom of nitrifiers. High velocity during the flood could cause increased nitrification and a switch the surface sediments from denitrification dominated to nitrification dominated (Kessler et al., 2015). It appears that maximum abundance of AOB occurring somewhat after the maximum of AOA suggesting that in this system, AOB followed the peak value in oxygen while AOA increased to maximum values when ammonium was at its maximum, as Luo (2014) found in sediments of JRE. There was a much higher increase in the copies of AOB than AOA during the Falling, particularly in high tide (Table S5). Tidal intrusion seems to support the ability of AOB to compete with AOA as the dominant niche.

This pattern of changing abundance of genes copies characteristic of nitrification was reflected in changes in the dissolved estuarine nitrogen. At the beginning of Flood ammonia-N increased somewhat more rapidly than nitrate (Fig. 2b) while DO during the Rising, remained at ~70 % saturation increasing to 80–100 % during the Falling (Fig. 3a). During the flood event in the JRE, there was evidence of strong nitrification which caused a decrease in δ^{15}N-NO_3 vs. δ^{18}O-NO_3 (Wang et al., 2021) and an increase in δ^{15}N-NH_4 (Lin et al., 2022). This is consistent with the inverse kinetic isotope effect of nitrification lead to higher δ^{15}N-NH_4 and lower δ^{15}N-NO_3 (Casciotti, 2009). Phytoplankton primary production in hypernutrified estuaries can compete with nitrification for ammonium (Kocum et al., 2002). However in the lower JRE, there was much reduced primary production as a result of the high concentration of SPM during the storms until ~10 days after the peak of storm discharge (Chen et al., 2018a). The concentration of nitrite remained relatively constant throughout the storm period with a small increase at the end of Ending (Fig. 2b). There was always a small accumulation of nitrite at Station E (Yan, 2012). This was a result of the dynamic between ammonia-oxidation, which had up to 20-fold different rates and precedes nitrite oxidation (Yan et al., 2019). However, during the storm the abundance of NOB (4.3×10^3 copies mL^{-1}) was close to the abundance of AOA and AOB (4.2×10^3 copies mL^{-1}) during the Rising which reduced the potential accumulation of nitrite in the water column (Table S4), particularly in high tide (Table S5).

4.3. The presence of the abundances of anaerobic N functional bacteria in the oxygen-rich water column of the JRE during the storm

This study showed the presence of denitrifying bacteria (*nar*G, *nir*S and *nod*), DNRA (*nrf*A) and anammox (*hzs*B) in the water column throughout the storm (Fig. 4). However, the presence of these gene abundances does not necessarily mean they are active since these types of microbes require anoxic or anaerobic conditions to be viable and reproduce (Galan et al., 2009; Handler et al., 2022; Hwang and Hanaki, 2000). The main location in the river system for anoxic conditions is the wastewater discharges such as domestic point sources and agricultural non-point sources (Palmer-Felgate et al., 2010). In the WJR this includes wastewater discharges from the city of Zhangzhou (Lin et al., 2022; Fig. 1). Anoxic conditions in the river are often associated surficial sediments near with such pollutant discharges with high labile organic matter contents (Yuan et al., 2021) and organic-rich sediment deposited in the upper estuary during normal flow (Chen et al., 2018b). During the Initial phase of the storm, when there was little or no resuspension in the upper estuary, and where 75 % of the sediments was >10 μm in size (Li et al., 2017), and there was only a moderate abundance of denitrifying bacteria in water column of Station E (Fig. 4d, e & f) dominantly associated with particulate matter (Fig. 5 d, e & f). As the river discharge increased in the Rising, there was a temporary increase in the number of all the denitrifying genes (Fig. 4). This could be due to increased erosion in the lower river catchment but an important additional source of particles which are likely to be rich in denitrifiers, is the resuspended sediments which was deposited during periods of normal flow (Table S5). This sediments is known to be anoxic close to the sediment-water interface (Chen et al., 2014; Gardner et al., 2009; Zhang et al., 2022). This source of denitrifying bacteria is likely to be associated with the organic-rich particulate matter (Eyre et al., 2013). During the peak of the storm (Rising and Falling) the fraction (Fig. 5 d, e &f) and abundance (Table S4) of FL bacteria increased for all types of denitrifying microbes. It is not known whether this was because of the injection of FL denitrifying bacteria from sediment pore waters or whether it was due to the attached microbes being detached from the surface of particles in the turbulent waters at the peak of the storm.

Although this study shows the amount and dynamic changes in the gene copies of denitrifying bacteria in the water column of the JRE during the storm, there is no direct evidence of what fraction of that population were viable and how many were dormant. These bacteria require suboxic/anoxic conditions to be active and thus it could be suggested that none of the free-living bacteria and most of the particle-attached bacteria were not active at this time, since the water they were carried with had oxygen levels of >70 % saturation (Fig. 3a). However, there is circumstantial evidence that this is too extreme a position. It is known from studies in the JRE and elsewhere that denitrification can occur in oxygenated waters associated with anoxic micro zones of labile organic matter in suspended particles (Reisinger et al., 2016; Xia et al., 2017; Zeng et al., 2018). The annual efficiency of N removal through denitrification/DIN load was 0–30 % in the JRE (Wu, 2013). Comparing the JRE with other China's estuaries, the denitrifier *nir*S genes and transcripts were more dominant in the JRE which has high levels of terrestrial nitrogen input (Dai et al., 2022). In the parallel study of N dynamics during this storm (Lin et al., 2022) there was a decrease in abundance of all denitrifiers in the late Rising and Falling as the amount of particulates decreased and the concentration of oxygen in the water column increased (Fig. 3a, Fig. 4). In the study on N dynamics

of the Jiulong river-estuary system during June 2019, it was not possible to estimate the amount of denitrification that had occurred in the system because that would have required a total N budget which was not carried out. However, it unlikely that active denitrification was a major process in the water column of the JRE because the amount of DO remained high (70–100 % saturation) and there remained 160–200 μmol NO_3-N L^{-1}. Further work is needed to determine accurately the amount of active denitrification in the water column and sediment during a storm.

The total number of bacterial counts, as measured by 16S rRNA, was relatively constant throughout the storm (Fig. 4i). However, this includes other heterotrophs which were neither nitrifiers nor denitrifiers.

5. Conclusions

Within the estuary the increased water discharge causes the freshwater/brackish water boundary to move downstream from its usual location during baseflow. It also causes the surficial sediment deposited during baseflow in the upper estuary to be resuspended, resulting in an additional injection of N chemical species (nitrate, ammonia and nitrite) and their associated N cycling microbes.

During normal baseflow when the ETM was located at Station E, ammonium which is dominantly sourced from domestic and agricultural waste water discharge was oxidised mainly by the marine nitrifying (AOA) microbe *Nitrosopelagicus*. As the discharge increased through the storm, the dominant ammonia-oxidizing archaea (AOA) changed to the riverine genus (*Nitrosotenuis*) with *Nitrosotalea*, while the marine genus, *Nitrosopumilus* decreased. By contrast the marine genus (*Nitrosomanas*) remained the dominant ammonia-oxidizing bacteria (AOB). Estuarine nitrifiers had higher abundance, weighted entropy and diversity during the Flood, suggesting that there was a bloom of nitrifier microbes caused by the high NH_4-N supplied from the river and the resuspended sediment pore waters, combined with the high DO (>70 % O_2 saturation) resulted in a bloom of active nitrifiers in free-living pattern. Direct evidence that nitrification was active came from observed modifications in the concentration of ammonium and nitrate in the water column and measured changes in the isotopic composition of DIN.

The numbers of N functional genes increased with increasing water discharge during the storm, and a larger fraction were associated with the <0.22 μm free-living fraction. The source of these anaerobic bacteria was likely to be waste-water discharges in the river and resuspended anoxic sediment from the upper estuary. It was not possible with the data obtained to estimate what fraction of these denitrifiers were active in the water column although previous studies have suggested that some denitrifiers can remain active in anaerobic microzones even though the overall water column has high levels of dissolved oxygen. Though it is likely that the amount of denitrification in the JRE was relatively low.

Previous work suggests that the much of the increased and altered flux of dissolved N caused by the changed microbial community passes through the estuary and reaches the coastal zone. The results of this study are important to develop science based management protocols to understand the nature and fluxes of anthropogenic N species through the river-estuary continuum to the coast. This is of particular relevance in systems such as the Jiulong river system where climate change is expected to increase the number and intensity of subtropical storms including those associated with ENSO.

CRediT authorship contribution statement

Jingjie Lin: Conceptualization, Data curation, Formal analysis, Investigation, Project administration, Software. **Anyi Hu:** Methodology. **Fenfang Wang:** Investigation. **Yiguo Hong:** Methodology, Software. **Michael D. Krom:** Conceptualization, Formal analysis. **Nengwang Chen:** Conceptualization, Funding acquisition, Project administration, Resources.

Data availability

No data was used for the research described in the article.

Declaration of competing interest

None.

Acknowledgements

This research was supported by the National Natural Science Foundation of China (No. 41676098; 51961125203). We thank all the students and Shuiying Huang who assisted with fieldwork, Xiuxiu Wang and Junou Du for their technical assistance.

Appendix A. Supplementary data

Supplementary data to this article can be found online at https://doi.org/10.1016/j.scitotenv.2022.160698.

References

Blanco, A.C., Nadaoka, K., Yamamoto, T., Kinjo, K., 2010. Dynamic evolution of nutrient discharge under stormflow and baseflow conditions in a coastal agricultural watershed in Ishigaki Island, Okinawa, Japan. Hydrol. Process. 24 (18), 2601–2616. https://doi.org/10.1002/hyp.7685.

Bollmann, A., Bar-Gilissen, M.J., Laanbroek, H.J., 2002. Growth at low ammonium concentrations and starvation response as potential factors involved in niche differentiation among ammonia-oxidizing bacteria. Appl. Environ. Microbiol. 68 (10), 4751–4757. https://doi.org/10.1128/aem.68.10.4751-4757.2002.

Brown, J.S., et al., 2013. Metals and bacteria partitioning to various size particles in ballona creek storm water runoff. Environ. Toxicol. Chem. 32 (2), 320–328. https://doi.org/10.1002/etc.2065.

Cao, W.Z., Hong, H.S., Yue, S.P., 2005. Modelling agricultural nitrogen contributions to the Jiulong River estuary and coastal water. Glob. Planet. Chang. 47 (2–4), 111–121. https://doi.org/10.1016/j.gloplacha.2004.10.006.

Casciotti, K.L., 2009. Inverse kinetic isotope fractionation during bacterial nitrite oxidation. Geochim. Cosmochim. Acta 73 (7), 2061–2076. https://doi.org/10.1016/j.gca.2008.12.022.

Chen, N.W., Wu, J.Z., Hong, H.S., 2012. Effect of storm events on riverine nitrogen dynamics in a subtropical watershed, southeastern China. Sci. Total Environ. 431, 357–365. https://doi.org/10.1016/j.scitotenv.2012.05.072.

Chen, N., Wu, J., Chen, Z., Lu, T., Wang, L., 2014. Spatial-temporal variation of dissolved N2 and denitrification in an agricultural river network, Southeast China. Agric. Ecosyst. Environ. 189, 1–10. https://doi.org/10.1016/j.agee.2014.03.004.

Chen, N.W., Krom, M.D., Wu, Y.Q., Yu, D., Hong, H.S., 2018a. Storm induced estuarine turbidity maxima and controls on nutrient fluxes across river-estuary-coast continuum. Sci. Total Environ. 628–629, 1108–1120. https://doi.org/10.1016/j.scitotenv.2018.02.060.

Chen, Y.N., Chen, N.W., Li, Y., Hong, H.S., 2018b. Multi-timescale sediment responses across a human impacted river-estuary system. J. Hydrol. 560, 160–172. https://doi.org/10.1016/j.jhydrol.2018.02.075.

Cheng, Z.Y., et al., 2021. GDGTs as indicators for organic-matter sources in a small subtropical river-estuary system. Org. Geochem. 153. https://doi.org/10.1016/j.orggeochem.2021.104180.

Chi, Z.F., et al., 2021. Deciphering edaphic bacterial community and function potential in a chinese delta under exogenous nutrient input and salinity stress. Catena 201. https://doi.org/10.1016/j.catena.2021.105212.

Cooper, A.B., 1983. Effect of storm events on benthic nitrifying activity. Appl. Environ. Microbiol. 46 (4), 957–960. https://doi.org/10.1128/aem.46.4.957-960.1983.

Dai, X.F., et al., 2022. Potential contributions of nitrifiers and denitrifiers to nitrous oxide sources and sinks in China's estuarine and coastal areas. Biogeosciences 19 (16), 3757–3773. https://doi.org/10.5194/bg-19-3757-2022.

Eyre, B.D., Maher, D.T., Squire, P., 2013. Quantity and quality of organic matter (detritus) drives N-2 effluxes (net denitrification) across seasons, benthic habitats, and estuaries. Glob. Biogeochem. Cycles 27 (4), 1083–1095. https://doi.org/10.1002/2013gb004631.

Fortin, S.G., Song, B., Anderson, I.C., 2021. Microbially mediated nitrogen removal and retention in the York River estuary. FEMS Microbiol. Ecol. 97 (9). https://doi.org/10.1093/femsec/fiab118.

Galan, A., et al., 2009. Anammox bacteria and the anaerobic oxidation of ammonium in the oxygen minimum zone off northern Chile. Deep-Sea Res. II Top. Stud. Oceanogr. 56 (16), 1125–1135. https://doi.org/10.1016/j.dsr2.2008.09.016.

Galloway, J.N., et al., 2008. Transformation of the nitrogen cycle: recent trends, questions, and potential solutions. Science 320 (5878), 889–892.

Gao, X.J., Chen, N.W., Yu, D., Wu, Y.Q., Huang, B.Q., 2018. Hydrological controls on nitrogen (ammonium versus nitrate) fluxes from river to coast in a subtropical region: observation and modeling. J. Environ. Manag. 213, 382–391. https://doi.org/10.1016/j.jenvman.2018.02.051.

Gardner, W.S., et al., 2009. Collection of intact sediment cores with overlying water to study nitrogen- and oxygen-dynamics in regions with seasonal hypoxia. Cont. Shelf Res. 29 (18), 2207–2213. https://doi.org/10.1016/j.csr.2009.08.012.

Handler, A.M., Suchy, A.K., Grimm, N.B., 2022. Denitrification and DNRA in urban accidental wetlands in Phoenix, Arizona. J. Geophys. Res. Biogeosci. 127 (2). https://doi.org/10.1029/2021jg006552.

Hou, L.J., et al., 2007. The effects of semi-lunar spring and neap tidal change on nitrification, denitrification and N2O vertical distribution in the intertidal sediments of the Yangtze estuary, China. Estuar. Coast. Shelf Sci. 73 (3), 607–616. https://doi.org/10.1016/j.ecss.2007.03.002.

Hou, L.J., et al., 2013. Anaerobic ammonium oxidation (anammox) bacterial diversity, abundance, and activity in marsh sediments of the Yangtze estuary. J. Geophys. Res. Biogeosci. 118 (3), 1237–1246. https://doi.org/10.1002/jgrg.20108.

Hwang, S., Hanaki, K., 2000. Effects of oxygen concentration and moisture content of refuse on nitrification, denitrification and nitrous oxide production. Bioresour. Technol. 71 (2), 159–165. https://doi.org/10.1016/S0960-8524(99)90068-8.

Jamieson, R., Joy, D.M., Lee, H., Kostaschuk, R., Gordon, R., 2005. Transport and deposition of sediment-associated Escherichia coli in natural streams. Water Res. 39 (12), 2665–2675. https://doi.org/10.1016/j.watres.2005.04.040.

Jeng, H.W.C., England, A.J., Bradford, H.B., 2005. Indicator organisms associated with stormwater suspended particles and estuarine sediment. J. Environ. Sci. Health A Tox. Hazard. Subst. Environ. Eng. 40 (4), 779–791. https://doi.org/10.1081/ese-200048264.

Kartal, B., et al., 2011. Molecular mechanism of anaerobic ammonium oxidation. Nature 479 (7371), 127–U159. https://doi.org/10.1038/nature10453.

Kessler, A.J., Cardenas, M.B., Cook, P.L.M., 2015. The Negligible Effect of Bed Form Migration on Denitrification in Hyporheic Zones of Permeable Sediments. 120(3), pp. 538–548. https://doi.org/10.1002/2014JG002852.

Kocum, E., Underwood, G.J.C., Nedwell, D.B., 2002. Simultaneous measurement of phytoplanktonic primary production, nutrient and light availability along a turbid, eutrophic UK east coast estuary (the colne Estuary). Mar. Ecol. Prog. Ser. 231, 1–12. https://doi.org/10.3354/meps231001.

Konneke, M., et al., 2005. Isolation of an autotrophic ammonia-oxidizing marine archaeon. Nature 437 (7058), 543–546. https://doi.org/10.1038/nature03911.

Li, R., Liang, J., Duan, H., Gong, Z., 2017. Spatial distribution and seasonal variation of phthalate esters in the Jiulong River estuary, Southeast China. Mar. Pollut. Bull. 122 (1), 38–46. https://doi.org/10.1016/j.marpolbul.2017.05.062.

Lin, J.J., et al., 2020. Impacts of human disturbance on the biogeochemical nitrogen cycle in a subtropical river system revealed by nitrifier and denitrifier genes. Sci. Total Environ. 746, 141139. https://doi.org/10.1016/j.scitotenv.2020.141139.

Lin, J.J., et al., 2022. Simultaneous observations revealed the non-steady state effects of a tropical storm on the export of particles and inorganic nitrogen through a river-estuary continuum. J. Hydrol. 606. https://doi.org/10.1016/j.jhydrol.2022.127438.

Luo, Z.X., 2014. Dynamics of ammonia-oxidizing archaea and bacteria in relation to nitrification along simulated dissolved oxygen gradient in sediment-water interface of the Jiulong river estuarine wetland, China. Environ. Earth Sci. 72 (7), 2225–2237. https://doi.org/10.1007/s12665-014-3128-6.

Meyer, R.L., Allen, D.E., Schmidt, S., 2008. Nitrification and denitrification as sources of sediment nitrous oxide production: a microsensor approach. Mar. Chem. 110 (1–2), 68–76. https://doi.org/10.1016/j.marchem.2008.02.004.

Nakatsu, C.H., Byappanahalli, M.N., Nevers, M.B., 2019. Bacterial community 16S rRNA gene sequencing characterizes riverine microbial impact on Lake Michigan. Front. Microbiol. 10, 12. https://doi.org/10.3389/fmicb.2019.00996.

Nevers, M.B., et al., 2020. Interaction of bacterial communities and indicators of water quality in shoreline sand, sediment, and water of Lake Michigan. Water Res. 178, 11. https://doi.org/10.1016/j.watres.2020.115671.

Palmer-Felgate, E.J., Mortimer, R.J.G., Krom, M.D., Jarvie, H.P., 2010. Impact of point-source pollution on phosphorus and nitrogen cycling in stream-bed sediments. Environ. Sci. Technol. 44 (3), 908–914. https://doi.org/10.1021/es902706r.

Pandey, C.B., et al., 2020. DNRA: a short-circuit in biological N-cycling to conserve nitrogen in terrestrial ecosystems. Sci. Total Environ. 738, 139710. https://doi.org/10.1016/j.scitotenv.2020.139710.

Reisinger, A.J., Tank, J.L., Hoellein, T.J., Hall Jr., R.O., 2016. Sediment, Water Column, and Open-channel Denitrification in Rivers Measured Using Membrane-inlet Mass Spectrometry. 121(5), pp. 1258–1274. https://doi.org/10.1002/2015JG003261.

Schloss, P.D., et al., 2009. Introducing mothur: open-source, platform-independent, community-supported software for describing and comparing microbial communities. Appl. Environ. Microbiol. 75 (23), 7537–7541. https://doi.org/10.1128/aem.01541-09.

Sorokin, D.Y., et al., 2012. Nitrification expanded: discovery, physiology and genomics of a nitrite-oxidizing bacterium from the phylum chloroflexi. ISME J. 6 (12), 2245–2256. https://doi.org/10.1038/ismej.2012.70.

Surbeck, C.Q., Jiang, S.C., Ahn, J.H., Grant, S.B., 2006. Flow fingerprinting fecal pollution and suspended solids in stormwater runoff from an urban coastal watershed. Environ. Sci. Technol. 40 (14), 4435–4441. https://doi.org/10.1021/es060701h.

Wagner, M., Rath, G., Koops, H.P., Flood, J., Amann, R., 1996. In situ analysis of nitrifying bacteria in sewage treatment plants. Water Sci. Technol. 34 (1–2), 237–244. https://doi.org/10.1016/0273-1223(96)00514-8.

Wang, X., et al., 2021. Isotopic constraint on the sources and biogeochemical cycling of nitrate in the Jiulong River estuary. J. Geophys. Res. Biogeosci. 126 (3). https://doi.org/10.1029/2020jg005850.

Wang, F.F., et al., 2022. Porewater exchange drives nutrient cycling and export in a mangrove-salt marsh ecotone. J. Hydrol. 606. https://doi.org/10.1016/j.jhydrol.2021.127401.

Warneke, S., et al., 2011. Nitrate removal, communities of denitrifiers and adverse effects in different carbon substrates for use in denitrification beds. Water Res. 45 (17), 5463–5475. https://doi.org/10.1016/j.watres.2011.08.007.

Wu, J.Z., 2013. Direct measurement of dissolved N-2 and denitrification along a subtropical river-estuary gradient, China. Mar. Pollut. Bull. 66 (1-2), 125–134. https://doi.org/10.1016/j.marpolbul.2012.10.020.

Xia, X.H., et al., 2017. Enhanced nitrogen loss from rivers through coupled nitrification-denitrification caused by suspended sediment. Sci. Total Environ. 579, 47–59. https://doi.org/10.1016/j.scitotenv.2016.10.181.

Yan, X.L., 2012. Distribution, fluxes and decadal changes of nutrients in the Jiulong River Estuary, Southwest Taiwan Strait. Chin. Sci. Bull. 57 (18), 2307–2318. https://doi.org/10.1007/s11434-012-5084-4.

Yan, X.L., et al., 2019. Biogeochemical dynamics in a eutrophic tidal estuary revealed by isotopic compositions of multiple nitrogen species. J. Geophys. Res. Biogeosci. 124 (7), 1849–1864. https://doi.org/10.1029/2018jg004959.

Yu, D., et al., 2019. Understanding how estuarine hydrology controls ammonium and other inorganic nitrogen concentrations and fluxes through the subtropical Jiulong River estuary, SE China under baseflow and flood-affected conditions. Biogeochemistry 142 (3), 443–466. https://doi.org/10.1007/s10533-019-00546-9.

Yu, D., Chen, N.W., Cheng, P., Yu, F.L., Hong, H.S., 2020. Hydrodynamic impacts on tidal-scale dissolved inorganic nitrogen cycling and export across the estuarine turbidity maxima to coast. Biogeochemistry 151 (1), 81–98. https://doi.org/10.1007/s10533-020-00712-4.

Yuan, X., Krom, M.D., Zhang, M.Z., Chen, N.W., 2021. Human disturbance on phosphorus sources, processes and riverine export in a subtropical watershed. Sci. Total Environ. 769. https://doi.org/10.1016/j.scitotenv.2020.144658.

Zeng, J., et al., 2018. Effects of particles on potential denitrification in the coastal waters of the beibu gulf in China. Sci. Total Environ. 624, 1274–1286. https://doi.org/10.1016/j.scitotenv.2017.12.192.

Zhang, M., et al., 2022. Effects of a storm on the transformation and export of phosphorus through a subtropical river-turbid estuary continuum revealed by continuous observation. J. Geophys. Res. Biogeosci. 127 (8). https://doi.org/10.1029/e2022JG006786.

Zou, D.Y., et al., 2020. Genomic characteristics of a novel species of ammonia-oxidizing archaea from the Jiulong River estuary. Appl. Environ. Microbiol. 86 (18). https://doi.org/10.1128/aem.00736-20.